33RD CONGRESS
OF THE INTERNATIONAL COUNCIL
OF THE AERONAUTICAL SCIENCES
STOCKHOLM, SWEDEN, 4-9 SEPTEMBER, 2022

ICAS 2022 SWEDEN

CONVEX PROGRAMMING-BASED OPTIMAL THREE-DIMENSIONAL MID-COURSE GUIDANCE WITH LOSSLESS CONVEXIFICATION

Cheol-Goo Jung[1], Chang-Hun Lee[2] & Min-Jea Tahk[3]

[1,2,3]Korea Advanced Institute of Science and Technology, Daejeon 34141, Republic of Korea

Abstract

The problem of optimal mid-course guidance of boost-glide missiles is studied. The final velocity is maximized with sequential second-order cone programming (SOCP). First, the missile flight phase is divided into boost and glide phases. Since the flight time of the glide phase is not fixed, this phase is reformulated using a new independent variable and the original problem is converted to a fixed final time problem. Then, dynamics is converted to input-affine form and partially linearized. To reduce an oscillation of input profiles, lossless convexification is performed to input terms consisting of a total angle-of-attack and bank angle. And the modified trust-region method is applied for robust convergence of solution with a roughly guessed initial trajectory.

Keywords: convex programming, lossless convexification, modified trust-region method

1. Introduction

Guidance law is one of the crucial parts of the missile GNC (Guidance, Navigation, and Control) loop. Guidance law determines the overall performance of the missile and a well-designed guidance law ensures that missiles accomplish the objective of the mission. Homing guidance or short-range missile guidance assumes that the current state of the missile is close to the collision course. Then, missile velocity change and aerodynamic forces are neglected. With these assumptions, dynamics are linearized around the collision triangle and linear optimal control theory is applied to derive a closed-form guidance law. This simple and effective method is used in deriving many guidance laws[1-4]. However, these assumptions are not reasonable for the mid-course guidance of medium- and long-range missiles. Velocity significantly changes in the mid-course phase because of thrust and aerodynamic drag. This time-varying velocity results in highly nonlinear dynamics. The linearization cannot reflect the original dynamics in guidance law and performance becomes degraded. Also, the assumption of collision course proximity cannot be used because deviation from the collision course can happen to maximize the ultimate objective. For example, a missile intentionally surges to a high altitude or low-density region to minimize the velocity loss. Because of these reasons, the previously mentioned guidance law cannot be applied to mid-course guidance even though they show good performance in a short-range scenario. As a result, a new methodology of deriving the guidance law is needed to satisfy many realistic constraints and nonlinear dynamics of medium- or long-range missiles.

To solve the obstacles to existing guidance, studies of trajectory optimization-based guidance are being attempted. The original optimal control problem is transcribed to the parameter optimization problem. This optimization problem is solved by the optimization algorithm such as interior-point optimizer (IPOPT) [5] or sparse nonlinear optimizer (SNOPT) [6]. And the obtained solution is used as a guidance law. This methodology can directly reflect the nonlinear dynamics and many realistic constraints. Because this methodology is an open-loop, the optimization solution should be obtained iteratively to compensate for the model uncertainty and disturbances. However, many nonlinear programming (NLP) algorithms are time-consuming to find a solution. Unpredictable computational time and lack of assured convergence are the main challenges in the application of optimization-based guidance in real-time [7]. The optimization solution should be rapidly obtained to be implemented in aerospace applications that generally have fast dynamics.

Convex programming is an appropriate alternative for solving computational time and convergence problems. Since convex programming problem has polynomial complexity, calculation time is predictable and bounded. Convex programming was applied to many aerospace applications such as landing problems [8,9], planetary entry [10], multiagent path planning [11], reentry of a rocket [12], missile trajectory optimization [13,14], and so on. this paper studies the convex programming-based optimal mid-course guidance of boost-glide missiles. Three-dimensional nonlinear missile dynamics are completely considered in problem formulation including thrust and aerodynamic forces. Control inputs are the total angle-of-attack and bank angle. First, the missile flight phase is divided into boost and glide phases. Thrust is only active in the boost phase and the thrust profile is fixed. Dynamics are converted to input-affine form and partially linearized. Then, lossless convexification is performed to input terms consisting of total angle-of-attack and bank angle. Input-affine form dynamics are partially linearized around the solution of the previous step except for the input term since the input term is already convexified. These dynamics are discretized with a pseudo-spectral method and the final velocity is maximized with second-order cone programming (SOCP).

The main contributions of this paper are two things. One is that the proposed convexification method speeds up the convergence rate with a minimal approximation. The main cause of slow convergence is the sequential linearization of dynamics. Because the SOCP algorithm can only solve a linear equality constraint, linearization of dynamics is inevitable. However, rapid convergence can be accomplished if the dynamics are partially linearized with the help of input affine form and input convexification. Secondly, the robustness of convergence is enhanced by a modified trust-region method. Auxiliary variables are used as a bound of trust-region and augmented to the original performance index. Numerical simulation shows that the proposed method can rapidly and robustly find the solution despite a roughly guessed initial trajectory compared to the constant trust-region method.

The remainder of the paper is organized as follows. In Section 2, a mathematical model of the missile is provided and the optimal control problem is formulated. The optimal control problem is reformulated into a convex programming problem in Section 3. Section 4 presents numerical simulation results, and conclusions are given in Section 5.

2. Problem Formulation

2.1 Missile Dynamic Model

Before providing missile dynamics, three assumptions are given. First, the control input immediately follows the command with an infinitely large bandwidth. Generally, the rotational dynamics of missiles is faster than translational dynamics. Since this paper aims to develop guidance law, attitude dynamics of total angle-of-attack and bank angle are neglected. Secondly, the missile is guided to the predicted impact point (PIP). With the help of station radar and data links, missiles can acquire the states of a target during the mid-course phase and calculate the PIP. Target can be treated as a fixed PIP point. Figure 1 presents a missile model in an inertial coordinate frame over the flat Earth. x, y, and h are downrange, crossrange, and altitude, respectively. V is the velocity of the missile, γ is a flight-path angle, and ψ is a heading angle. Input variables α and ϕ are total angle-of-attack and bank angle. D and L are aerodynamic drag and lift. Finally, m and T are mass of the missile and thrust that is aligned with body longitudinal axis of the missile body.

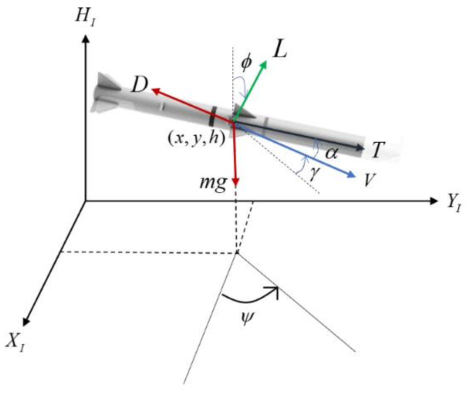

Figure 1 – Missile dynamic model.

Referring to the definition of variables, three-dimensional missile dynamics is as follows:

$$\dot{x} = V\cos\gamma\sin\psi \tag{1a}$$

$$\dot{y} = V\cos\gamma\sin\psi \tag{1b}$$

$$\dot{h} = V\sin\gamma \tag{1c}$$

$$\dot{V} = \frac{T\cos\alpha - D}{m} - g\sin\gamma \tag{1d}$$

$$\dot{\gamma} = \frac{(T\sin\alpha + L)\cos\phi}{mV} - \frac{g\cos\gamma}{V} \tag{1e}$$

$$\dot{\psi} = \frac{(T\sin\alpha + L)\sin\phi}{mV\cos\gamma} \tag{1 f}$$

Aerodynamic drag D and lift L are modeled using typical drag polar as (2-3). C_{D0} is the zero-lift drag coefficient, K is induced drag and $C_{L\alpha}$ is lift slope. S_{ref} is reference area, and q is dynamic pressure. Air density is approximated with an exponential function of altitude as (6).

$$D = qS_{ref}(C_{D0} + KC_L^2) \tag{2}$$

$$L = qS_{ref}C_L \tag{3}$$

$$C_L = C_{L\alpha}\alpha \tag{4}$$

$$q = \frac{1}{2}\rho V^2 \tag{5}$$

$$\rho = \rho_0 e^{-h/h_s} \tag{6}$$

Thrust is turned on in the boost phase with predetermined burn time and turned off in the glide phase. The thrust profile and mass of the missile are modeled as (7-8).

$$T = \begin{cases} T_0 & 0 < t \le t_{burn} \\ 0 & t_{burn} < t \le t_f \end{cases} \tag{7}$$

$$m = \begin{cases} m_0 - \dot{m}t & 0 < t \le t_{burn} \\ m_0 - \dot{m}t_{burn} & t_{burn} < t \le t_f \end{cases} \tag{8}$$

where $\dot{m}$ is fuel consumption rate, t_{burn} is burn time of thrust, and t_f is terminal time.

2.2 Constraints and Performance Index

In this subsection, constraints and performance index are provided. Since an excessive total angle-of-attack may cause the missile to stall or become unstable, the total angle-of-attack is bounded by the maximum value during the flight time. Furthermore, the total angle-of-attack is defined as a positive sign. This constraint is presented as

$$0 \le \alpha \le \alpha_{\max} \tag{9}$$

To nullify the miss distance, the terminal constraint of position(PIP) should be imposed.

$$x(t_f) = x_f,\ y(t_f) = y_f,\ h(t_f) = h_f \tag{10}$$

Furthermore, a specific impact angle(flight-path angle and heading angle) is required to increase the effectiveness of the warhead and mitigate the ground clutter effect.

$$\gamma(t_f) = \gamma_f, \psi(t_f) = \psi_f \tag{11}$$

For sufficient maneuverability in homing phase, terminal velocity is maximized. The performance index is set as

$$J = -V(t_f) \tag{12}$$

Now, missile dynamics, constraints, and performance index yield the optimal control problem:

Problem A :

minimize $-V(t_f)$

subject to (1), (9), (10-11)

Problem A has highly nonlinear dynamics and input constraints. With suitable reformulation, this optimal control problem can be handled with parameter optimization such as convex programming. In parameter optimization, original continuous-time domain dynamics is discretized and solved by the optimization algorithm. The detailed procedure is explained in the next section.

3. Problem Reformulation into Convex Programming Form

3.1 New Independent Variable

In this section, Problem A is reformulated into a suitable form that can be solved by convex programming. Firstly, missile dynamics is reformulated using a change of independent variable. Dynamics (1) can be separated into two phases: boost and glide phase. The time interval of the boost phase is defined and that of the glide phase is not. For the discretization of dynamics, the independent variable must be monotonically increasing(or decreasing) and have a fixed boundary. However, the terminal time of the glide phase is not fixed. To address this problem, a new independent variable $\tau \in [0,1]$ and time scale variable $\eta(= t_f - t_{burn})$ is introduced. The time t of the glide phase is parameterized with τ and η as

$$t = t_{burn} + \eta\tau, \ (0 < \tau \le 1) \tag{13}$$

and the independent variable of the boost phase is still the same. The relationship between t and τ is graphically presented in Figure 2. It may seem unnatural to use a differently scaled independent variable for each phase. However, separated dynamics can be handled using a linkage condition between two phases. The utility of this method becomes clear in the following subsections.

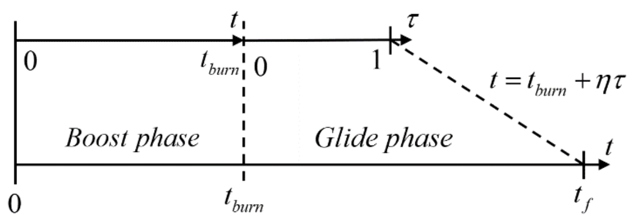

Figure 2 – Relationship between time and new independent variable.

Now, reformulated dynamics for the glide phase can be derived using the differential relationship between t and τ, i.e. $dt = \eta d\tau$, as follows:

$$\frac{dx}{d\tau} = \eta V \cos\gamma \sin\psi \tag{14a}$$

$$\frac{dy}{d\tau} = \eta V \cos\gamma \sin\psi \tag{14b}$$

$$\frac{dh}{d\tau} = \eta V \sin\gamma \tag{14c}$$

$$\frac{dV}{d\tau} = \eta\left(\frac{T\cos\alpha - D}{m} - g\sin\gamma\right) \tag{14d}$$

$$\frac{d\gamma}{d\tau} = \eta\left(\frac{(T\sin\alpha + L)\cos\phi}{mV} - \frac{g\cos\gamma}{V}\right) \tag{14e}$$

$$\frac{d\psi}{d\tau} = \eta\left(\frac{(T\sin\alpha + L)\sin\phi}{mV\cos\gamma}\right) \tag{14 f}$$

Original missile dynamics is separated into two dynamics, (1) for the boost phase and (14) for the glide phase. The original free terminal time problem can be converted to an equivalent fixed terminal time problem using (14) with an additional optimization variable η. The terminal condition and performance index are reformulated using τ as

$$x(\tau=1) = x_f,\; y(\tau=1) = y_f,\; h(\tau=1) = h_f \tag{15}$$

$$\gamma(\tau=1) = \gamma_f,\, \psi(\tau=1) = \psi_f \tag{16}$$

$$J = -V(\tau=1) \tag{17}$$

3.2 Partial Linearization

Second-order cone programming can only solve the specific form of problems: 1) performance index of a linear function, 2) linear equality constraints, and 3) second-order cone inequality constraints. Since missile dynamics correspond to equality constraints, linearization of nonlinear dynamics is necessary. Before performing linearization, the dynamics is converted to input-affine form. To factor out input variable from dynamics, total angle-of-attack terms are approximated with second-order Tayler series as

$$\sin\alpha \approx \alpha,\; \cos\alpha \approx 1 - 0.5\alpha^2 \tag{18}$$

This approximation is reasonable since the missile generally uses a small total angle-of-attack during the mid-course phase to reduce induced drag and conserve energy. Furthermore, the total angle-of-attack is bounded by the maximum value from (9). Then, input terms are replaced by

$$u_1 = \alpha\cos\phi \tag{19}$$

$$u_2 = \alpha\sin\phi \tag{20}$$

$$u_3 = \alpha^2 \tag{21}$$

Since these new input variables u_1, u_2, and u_3 are not independent, the following constraint should be added

$$u_1^2 + u_2^2 = u_3 \tag{22}$$

Then, nonlinear dynamics (1) and (14) are converted into the following input-affine form:

$$\frac{d\mathbf{z}}{dt} = \mathbf{f}(\mathbf{z}) + \mathbf{b}(\mathbf{z})\mathbf{u}, \quad t \in \left(0, t_{burn}\right] \tag{23a}$$

$$\frac{d\mathbf{z}}{d\tau} = \eta\left(\mathbf{f}(\mathbf{z}) + \mathbf{b}(\mathbf{z})\mathbf{u}\right), \quad \tau \in \left(0, 1\right] \tag{23b}$$

$$where \ \ \mathbf{z} = \left[x \ y \ h \ V \ \gamma \ \psi\right]^T, \ \mathbf{u} = \left[u_1 \ u_2 \ u_3\right]^T$$

$$\mathbf{f}(\mathbf{z}) = \begin{bmatrix} V\cos\gamma\cos\psi \\ V\cos\gamma\sin\psi \\ V\sin\gamma \\ \dfrac{T - qS_{ref}C_{D0}}{m} - g\sin\gamma \\ -\dfrac{g\cos\gamma}{V} \\ 0 \end{bmatrix}, \ \mathbf{b}(\mathbf{z}) = \begin{bmatrix} 0_{3\times1} & 0_{3\times1} & 0_{3\times1} \\ 0 & 0 & \dfrac{-0.5T - qS_{ref}KC_{L\alpha}^2}{m} \\ \dfrac{T + qS_{ref}C_{L\alpha}}{mV} & 0 & 0 \\ 0 & \dfrac{T + qS_{ref}C_{L\alpha}}{mV\cos\gamma} & 0 \end{bmatrix}$$

(23a) and (23b) are partially linearized along $\mathbf{z}^k$ and η^k which are the optimal solution at k th iteration.

$$\frac{d\mathbf{z}}{dt} = \mathbf{a}(\mathbf{z}^k)\mathbf{z} + \mathbf{b}(\mathbf{z}^k)\mathbf{u} + \mathbf{c}(\mathbf{z}^k), \quad t \in \left(0, t_{burn}\right] \tag{24a}$$

$$\frac{d\mathbf{z}}{d\tau} = \eta^k\mathbf{a}(\mathbf{z}^k)\mathbf{z} + \eta^k\mathbf{b}(\mathbf{z}^k)\mathbf{u} + \mathbf{f}(\mathbf{z}^k)\eta + \mathbf{d}(\mathbf{z}^k, \eta^k), \quad \tau \in \left(0, 1\right] \tag{24b}$$

$$where \ \ \mathbf{a}(\mathbf{z}^k) = \frac{\partial\mathbf{f}(\mathbf{z}^k)}{\partial\mathbf{z}}, \ \ \mathbf{c}(\mathbf{z}^k) = \mathbf{f}(\mathbf{z}^k) - \frac{\partial\mathbf{f}(\mathbf{z}^k)}{\partial\mathbf{z}}\mathbf{z}^k, \ \ \mathbf{d}(\mathbf{z}^k, \eta^k) = -\eta^k\frac{\partial\mathbf{f}(\mathbf{z}^k)}{\partial\mathbf{z}}\mathbf{z}^k$$

(24) shows that linearization is not performed in the input term $\mathbf{b}(\mathbf{z})\mathbf{u}$ and $\eta\mathbf{b}(\mathbf{z})\mathbf{u}$. This method can reduce the oscillating profile of the input solution and results in fast convergence[15]. To confine the change of states $\mathbf{z}^k$ at each iteration, a trust-region constraint is imposed.

$$\left|\mathbf{z} - \mathbf{z}^k\right| \le \boldsymbol{\delta} \tag{25}$$

where $\boldsymbol{\delta}$ defines the radius of the trust-region of each component of states.

3.3 Lossless Convexification

Even though the nonlinear missile dynamics is linearized, the admissible input set is not convex because of constraint (22). From (9) and (22), the admissible input set is presented as follows

$$\Sigma = \left\{(u_1, u_2, u_3) \middle| \, u_1^2 + u_2^2 = u_3, 0 \le u_3 \le \alpha_{\max}^2 \right\} \tag{26}$$

Figure 3a graphically shows the admissible input set of u_1, u_2 and u_3. This nonconvex admissible input set can be easily convexified using convex relaxation[7] as

$$\tilde{\Sigma} = \mathbf{conv}\Sigma = \left\{(u_1, u_2, u_3) \middle| \, u_1^2 + u_2^2 \le u_3, 0 \le u_3 \le \alpha_{\max}^2 \right\} \tag{27}$$

where **conv** denotes the convex hull. Convex hall of S is defined by the smallest convex set including S.

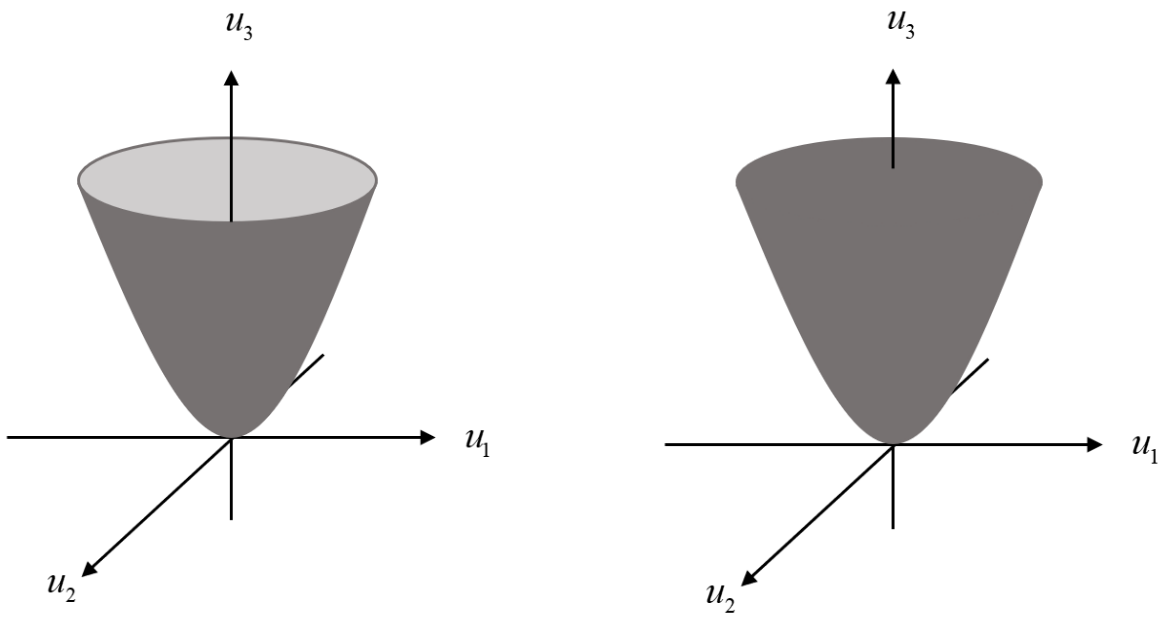

a) Nonconvex admissible set b) Convexified admissible set

Figure 3 – Nonconvex and convexified admissible input sets.

Now, Problem B is presented as

Problem B :

minimize $-V(\tau = 1)$

subject to (15-16), (24), (25), (27)

Solution space for Problem B widens by applying convex relaxation (27). However, it can be proved that the optimal solution to Problem B always satisfies equality (26), which means lossless convexification. This fact can be shown using optimal control theory. Moreover, it can be intuitively explained. The third column of $\mathbf{b}(\mathbf{z})$ in (23) multiplied by u_3 influences the velocity rate. Because the sign of this term is negative, it is obvious that u_3 should be minimized at all times to maximize the terminal velocity.

3.4 Discretization and Modified Trust-Region Method

The continuous-time domain Problem B is discretized to a finite-dimensional parameter optimization problem. Linear dynamics of (24) is transcribed using the pseudo-spectral method. The pseudo-spectral method is one of the discretization methods such as the trapezoidal and Hermite-Simpson methods. The characteristic of this method is that states and inputs are approximated with a global interpolation function using orthogonal collocation points. In this paper, Legendre-Gauss-Radau (LGR) collocation points are used as nodes. A detailed description of the pseudo-spectral method can be found in many papers[16-19]. In this paper, only the result is presented.

$$\mathbf{D}_{1,i} \cdot \mathbf{Z}_1 = k_1 \left[\mathbf{a}(\mathbf{z}_{1,i}^k)\mathbf{z}_{1,i} + \mathbf{b}(\mathbf{z}_{1,i}^k)\mathbf{u}_{1,i} + \mathbf{c}(\mathbf{z}_{1,i}^k) \right],\ i = 0,1,\ldots,N_1 \tag{28a}$$

$$\mathbf{D}_{2,i} \cdot \mathbf{Z}_1 = k_2 \left[\eta^k \mathbf{a}(\mathbf{z}_{2,i}^k)\mathbf{z}_{2,i} + \eta^k \mathbf{b}(\mathbf{z}_{2,i}^k)\mathbf{u}_{2,i} + \mathbf{f}(\mathbf{z}_{2,i}^k)\eta + \mathbf{d}(\mathbf{z}_{2,i}^k, \eta^k) \right],\ i = 0,1,\ldots,N_2 \tag{28b}$$

$$where\ \ \mathbf{Z}_j = \left[\mathbf{z}_{j,0}^T\, \mathbf{z}_{j,1}^T \cdots \mathbf{z}_{j,N_j}^T \right]^T,\ \ \mathbf{U}_j = \left[\mathbf{u}_{j,0}^T\, \mathbf{u}_{j,1}^T \cdots \mathbf{u}_{j,N_j}^T \right]^T,\ k_1 = \frac{t_{bunr}}{2},\ k_2 = \frac{1}{2}$$

In (28), 1 and 2 denote the boost and glide phases, respectively. N_i is the number of collocation points. $\mathbf{Z}_{j,i}$ and $\mathbf{U}_{j,i}$ denotes the state and input values of j the node. $\mathbf{D}_{j,i}$ is a differentiation matrix that can be derived using Lagrange polynomial and collocation points[16].

(28) only provides the state/input relationship within each phase. For connecting two phases, linkage conditions are added. This condition connects the terminal value of the boost phase and the initial value of the glide phase.

$$\mathbf{z}_{1,N_1} = \mathbf{z}_{2,0} \tag{29}$$

The size of the trust-region (25) should be properly selected. Otherwise, the problem becomes infeasible or the solution diverges with a roughly estimated initial trajectory. To alleviate this difficulty, the constant trust-region is replaced by following quadratic trust-region constraint using an auxiliary variable $s_{j,i}$

$$\left[\mathbf{z}_{j,i} - \mathbf{z}^k_{j,i}\right]^T \left[\mathbf{z}_{j,i} - \mathbf{z}^k_{j,i}\right] \le s_{j,i}, \quad j = 1, 2 \ and \ i = 0, 1, ..., N_j \tag{30}$$

The total sum of $s_{j,i}$ is multiplied by w_t and augmented to the original performance index.

$$\bar{J} = -V(\tau = 1) + w_t \sum_{j=1}^{2} \sum_{i=0}^{N_j} s_{j,i} \tag{29}$$

w_t should be selected as a sufficiently small value not to disturb the original objective of maximizing terminal velocity. This modified trust-region method prevents the problem from being infeasible. Furthermore, proper w_t can be easily found after a little trial and error. Finally, a second-order cone programming problem is presented.

Problem C :

minimize $\bar{J} = -V(\tau = 1) + w_t \sum_{j=1}^{2} \sum_{i=0}^{N_j} s_{j,i}$

subject to (15-16), (27), (28), (30)

An optimal solution can be obtained by sequentially solving Problem C until the convergence condition is satisfied. A sequential convex programming algorithm is consists of the following steps:

Step 1) Initial guess: Initial guess of states $\mathbf{z}^0_{j,i}$ at every node and time scale variable η^0 are selected. And set $k = 1$.

Step 2) Solving convex programming problem: For $k \ge 1$, a new optimal solution $\{\mathbf{z}^k, \mathbf{u}^k, \eta^k\}$ is obtained by solving Problem C using the previous solution $\{\mathbf{z}^{k-1}, \mathbf{u}^{k-1}, \eta^{k-1}\}$.

Step 3) Terminal condition: If the following convergence condition is satisfied,

$$\max_{i,j} \left| \mathbf{z}^k_{j,i} - \mathbf{z}^{k-1}_{j,i} \right| < \boldsymbol{\varepsilon}$$

finish the iteration and the optimal solution is $\{\mathbf{z}^k, \mathbf{u}^k, \eta^k\}$. Otherwise, go to step2. $\boldsymbol{\varepsilon}$ can be selected as an appropriate small value.

States and time scale variable should be initialized to start the sequential convex programming. Here we use a simple way to select the initial values. A line connecting the initial and terminal position is selected as an initial trajectory of x_0, y_0, and h_0. Initial velocity V_0, flight-path angle γ_0, and heading angle ψ_0 are set as $2V_0$, zero, and arctan(y_f / x_f) at every node, respectively. The time scale variable η_0 is initialized with $l/(2V_0)$, where l is the length of the line connecting the initial and terminal position.

4. Numerical Simulation

In this section, the proposed method is applied to the mid-course guidance of the boost-glide missile. Used parameters are summarized in Table 1.

Table 1 – Simulation parameters

Parameter	Value
Thrust, T_0	8 kN
Fuel consumption rate, $\dot{m}$	3.5 kg/s
Burn time, t_{burn}	10 sec
Maximum angle-of-attack, $\alpha_{\max}$	15°
Weight of performance index, w_{trust}	0.025
Number of nodes, N_1, N_2	20
Convergence condition parameter, $\boldsymbol{\varepsilon}$	[30m, 30m, 30m, 3m/s, 0.5°, 0.5°]

To verify the validity of the proposed method, three different engagement scenarios are considered. The initial and terminal conditions of each scenario are shown in Table 2. Firstly, the convergence characteristics of the proposed method are discussed. Figure 4 shows the convergence process of the first scenario. Even though the states and time scale variables are roughly initialized, the solution rapidly converges to a steady value with 6 iterations. It only takes 0.13 ~ 0.15 sec to solve the Problem C at each iteration with Intel Core i5-12500 at 3.00 GHz. Even though the optimality of the converged solution cannot be proved in sequential convex programming, we can intuitively verify the optimality by graphically observing the convergence process. Figure 4a presents the flight trajectory at each iteration. After a large movement at the first iteration, the trajectory gradually converges to a specific profile. Figure 4d shows the maximum change of state out of all node points. Change of every state converges to zero which means states do not need to vary any longer for minimizing the performance index. As a result, the augmented term of (29) becomes a negligibly small value compared to the original performance index of terminal velocity. Furthermore, Figures 4b and 4c show the stable convergence of the performance index and time scale variable. And Figure 5 visually shows the lossless convexification: inequality constraint of (27) is active for all node points.

Table 2 – Initial and terminal conditions

Scenario	Initial conditions ($x_0, y_0, h_0, V_0, \gamma_0, \psi_0$), (km, km, km, m/s, °, °)	Terminal conditions ($x_f, y_f, h_f, V_f, \gamma_f, \psi_f$), (km, km, km, m/s, °, °)
1	(0, 0, 5, 350, 0, 0)	(40, 5, 5, free, -10, free)
2	(0, 0, 5, 350, 0, 0)	(45, 7, 5, free, -10, free)
3	(0, 0, 5, 350, 0, 0)	(50, 9, 5, free, -10, free)

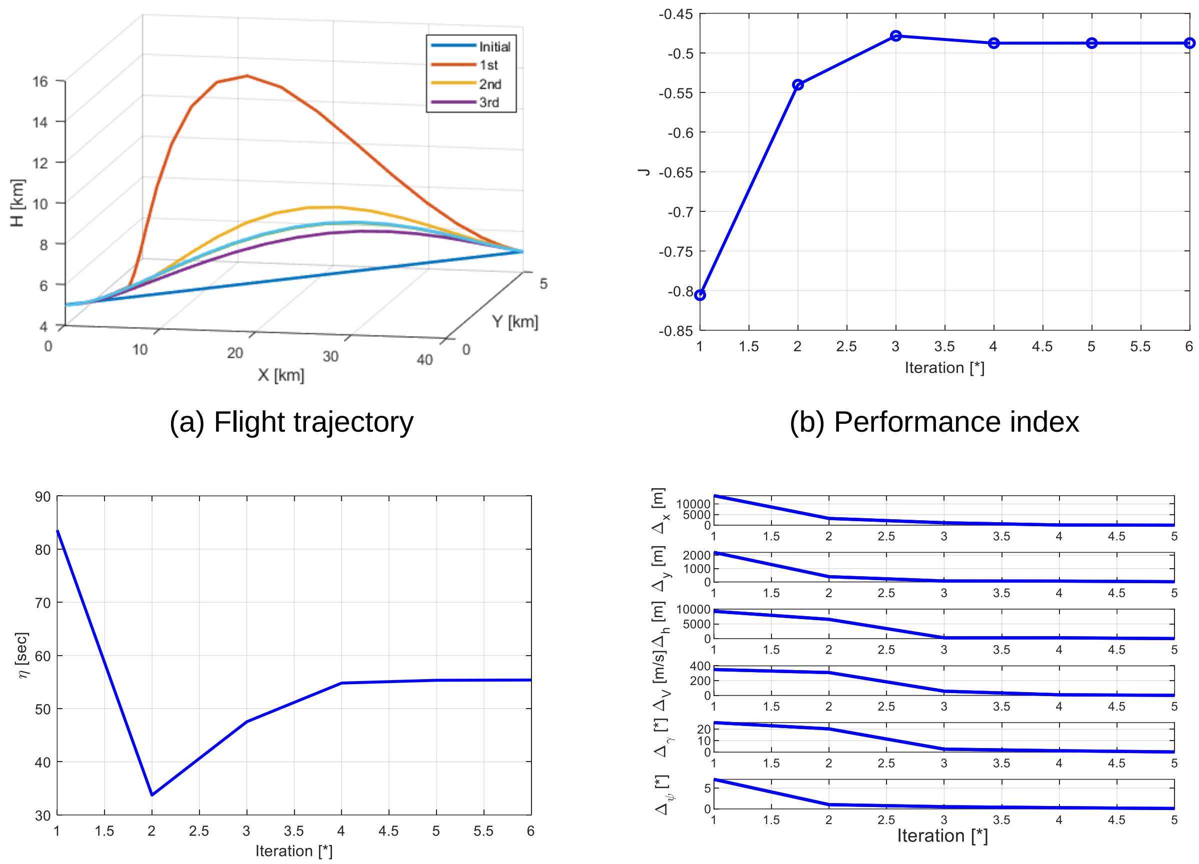

(a) Flight trajectory

(b) Performance index

(c) Time scale variable

(d) Change of states

Figure 4 – Convergence of the proposed method.

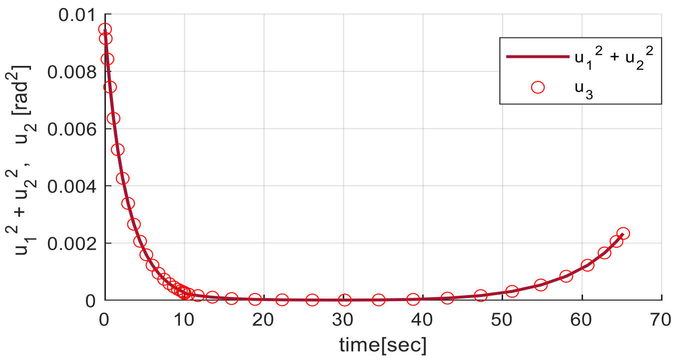

Figure 5 – Lossless convexification.

The converged trajectories of each scenario are plotted in Figure 6 and the red circle denotes the launch point. This figure shows a smooth flight trajectory for all scenarios, and the missile impacts the targeted terminal positions. It can be seen that the longer the range, the higher the altitude. Figure 7 presents the missile velocity which shows a similar profile during the boost phase. However, scenario 3 shows the smallest velocity during the glide time to reach the highest altitude and the longest range except for the terminal phase. Figures 8 and 9 show the flight-path angle and heding angle. These figures indicate that the specified terminal flight-path angle is satisfied for all scenarios. And heading angle shows the high change rate at the beginning and gradually converges to the terminal heading angle which is not specified. Finally, Figures 10 and 11 present the total angle-of-attack and bank angle, which show the smooth control input profiles. The original input value can be obtained by inversely solving (19-21) for the total angle-of-attack and bank angle after the solution converges. The missile uses a small total angle-of-attack less than 7 deg during its entire flight. The bank angle rapidly changes after the boost phase. Then, it decreases after reaching the peak and asymptotically converges to zero.

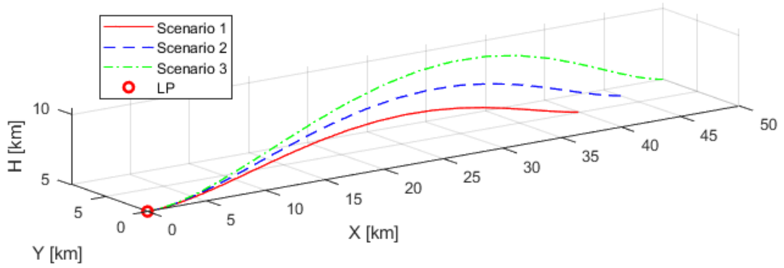

Figure 6 – Three-dimensional flight trajectories.

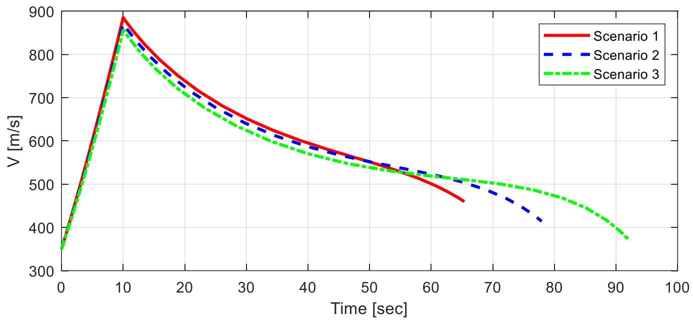

Figure 7 – Velocity profiles.

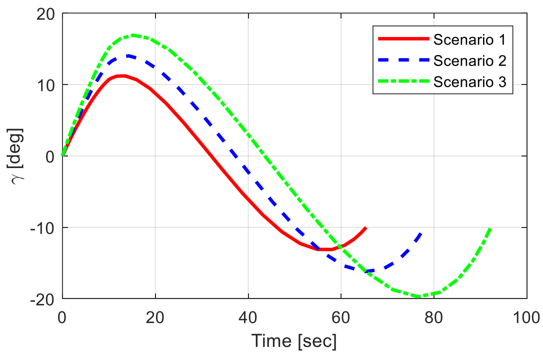

Figure 8 – Flight-path angle profiles.

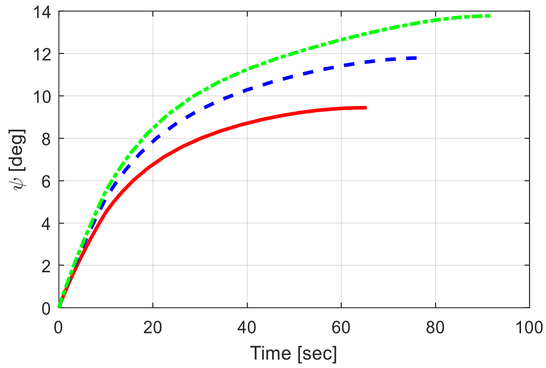

Figure 9 – Heading angle profiles.

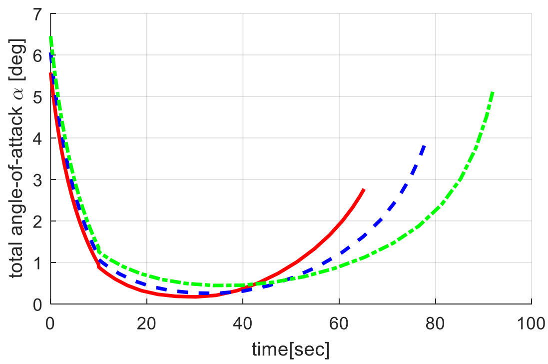

Figure 10 – Total angle-of-attack profiles.

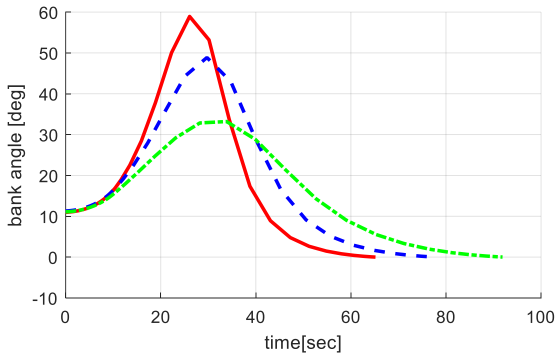

Figure 11 – Bank angle profiles.

Finally, an additional simulation is performed with the same initial and terminal condition as Table 2 except for the terminal constraint of a heading angle of 20°. Figure 13 shows the heading angle profile. A terminal heading angle of 20° is satisfied for all scenarios. Figure 14 and 15 present a similar total angle-of-attack profile to Figure 10. However, the bank angle is larger than Figure 11 and does not converge to zero to satisfy the terminal heading angle constraint. This result indicates that more input is needed to satisfy more constraints.

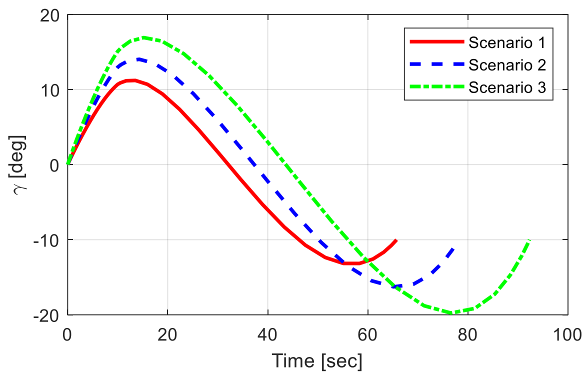

Figure 12 – Total angle-of-attack profiles with terminal heading angle.

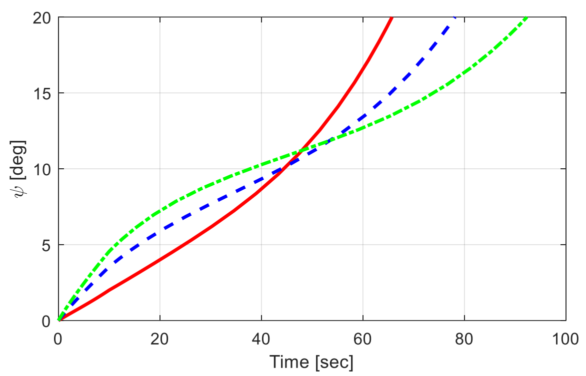

Figure 13 – Flight-path angle with terminal heading angle.

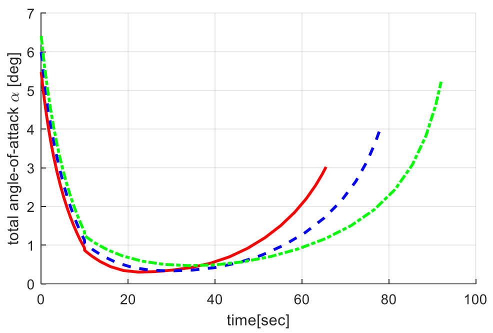

Figure 14 – Total angle-of-attack profiles with terminal heading angle.

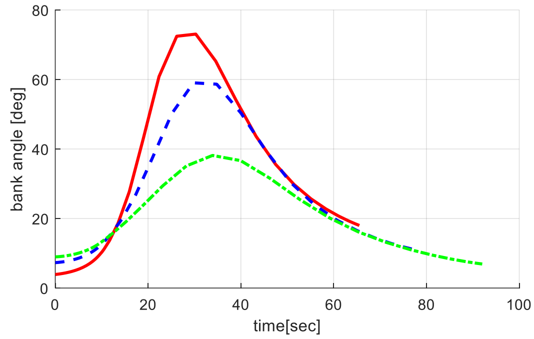

Figure 15 – Bank angle profiles with terminal heading angle.

5. Conclusion

This paper presents a convex programming-based method to solve the mid-course guidance problem of the boost-glide missile. The original nonlinear optimal control problem is reformulated using a new independent variable and time scale variable. Then, this reformulated problem is converted to a sequential convex programming problem with the help of lossless convexification. To ensure robust and fast convergence even under roughly given initial trajectories, a modified trust-region method is proposed. The proposed method effectively solves the guidance problem without infeasibility and slow convergence problems. Numerical simulation applied to the mid-course guidance problem of various scenarios provides obvious effectiveness of the proposed method.

6. Contact Author Email Address

Chang-Hun Lee (corresponding author): lckdgns@kaist.ac.kr

7. Copyright Statement

8. Acknowledgment

This work was supported by the Theater Defense Research Center funded by the Defense Acquisition Program Administration under Grant UD200043CD.

References

[1] Ryoo, Chang-Kyung, Hangju Cho, and Min-Jea Tahk. Optimal guidance laws with terminal impact angle constraint. *Journal of Guidance, Control, and Dynamics*, Vol. 28, No. 4, pp 724-732, 2005.

[2] Jeon, In-Soo, Jin-Ik Lee, and Min-Jea Tahk. Impact-time-control guidance law for anti-ship missiles. *IEEE Transactions on control systems technology*, Vol. 14, No. 2, pp 260-266, 2006.

[3] White, Brian, et al. Optimal guidance solution for impact angle control based on linearization about collision triangle. *IFAC Proceedings*, Vol. 44, No. 1 pp 3909-3914, 2011.

[4] Lee, Jin-Ik, In-Soo Jeon, and Min-Jea Tahk. Guidance law to control impact time and angle. *IEEE Transactions on Aerospace and Electronic Systems,* Vol. 43, No. 1, pp 301-310, 2007.

[5] Gill, Philip E., Walter Murray, and Michael A. Saunders. SNOPT: An SQP algorithm for large-scale constrained optimization. *SIAM review,* Vol. 47, No. 1, pp 99-131, 2005.

[6] Wächter, Andreas, and Lorenz T. Biegler. On the implementation of an interior-point filter line-search algorithm for large-scale nonlinear programming. *Mathematical programming,* Vol. 106, No. 1, pp 25-57, 2006.

[7] Liu, Xinfu, Ping Lu, and Binfeng Pan. Survey of convex optimization for aerospace applications. *Astrodynamics,* Vol. 1, No. 1, pp 23-40, 2017.

[8] Blackmore, Lars, Behçet Açikmeşe, and Daniel P. Scharf. Minimum-landing-error powered-descent guidance for Mars landing using convex optimization. *Journal of guidance, control, and dynamics,* Vol. 33, No. 4, pp 1161-1171, 2010.

[9] Sagliano, Marco. Pseudospectral convex optimization for powered descent and landing. *Journal of guidance, control, and dynamics,* Vol. 41, No. 2, pp 320-334, 2018.

[10] Wang, Zhenbo, and Michael J. Grant. Constrained trajectory optimization for planetary entry via sequential convex programming. *Journal of Guidance, Control, and Dynamics,* Vol. 40, No. 10, pp 2603-2615, 2017.

[11] Chen, Yufan, Mark Cutler, and Jonathan P. How. Decoupled multiagent path planning via incremental sequential convex programming. *2015 IEEE International Conference on Robotics and Automation (ICRA)*. IEEE, 2015.

[12] HWANG, JUNSUB, and Jaemyung Ahn. Integrated Optimal Guidance for Reentry and Landing of a VTVL Rocket Using Multi-phase Pseudo-spectral Convex Optimization. *Asia-Pacific International Symposium on Aerospace Technology*. Korean Society for Aeronautical and Space Sciences, 2021.

[13] Roh, Heekun, et al. L1 Penalized Sequential Convex Programming for Fast Trajectory Optimization: With Application to Optimal Missile Guidance. *International Journal of Aeronautical and Space Sciences,* Vol. 21, No. 2, pp 493-503, 2020.

[14] Kwon, Hyuck-Hoon, and Han-Lim Choi. A convex programming approach to mid-course trajectory optimization for air-to-ground missiles. *International Journal of Aeronautical and Space Sciences,* Vol. 21, No. 2, pp 479-492, 2020.

[15] Liu, Xinfu, Zuojun Shen, and Ping Lu. Entry trajectory optimization by second-order cone programming. *Journal of Guidance, Control, and Dynamics,* Vol. 39, No. 2, pp 227-241, 2016.

[16] Garg, Divya, et al. An overview of three pseudospectral methods for the numerical solution of optimal control problems. 2017.

[17] Benson, David. *A Gauss pseudospectral transcription for optimal control*. Diss. Massachusetts Institute of Technology, 2005.

[18] Sagliano, Marco. Pseudospectral convex optimization for powered descent and landing. *Journal of guidance, control, and dynamics,* Vol. 41, No. 2, pp 320-334, 2018.

[19] Darby, Christopher L., William W. Hager, and Anil V. Rao. An hp-adaptive pseudospectral method for solving optimal control problems. *Optimal Control Applications and Methods,* Vol.32, No.4, pp 476-502, 2011.